

# Remote Sensing and Earthquake Damage Detection Using Optical Images

Masashi Matsuoka  
Tokyo Institute of Technology

1

## What is Remote Sensing?



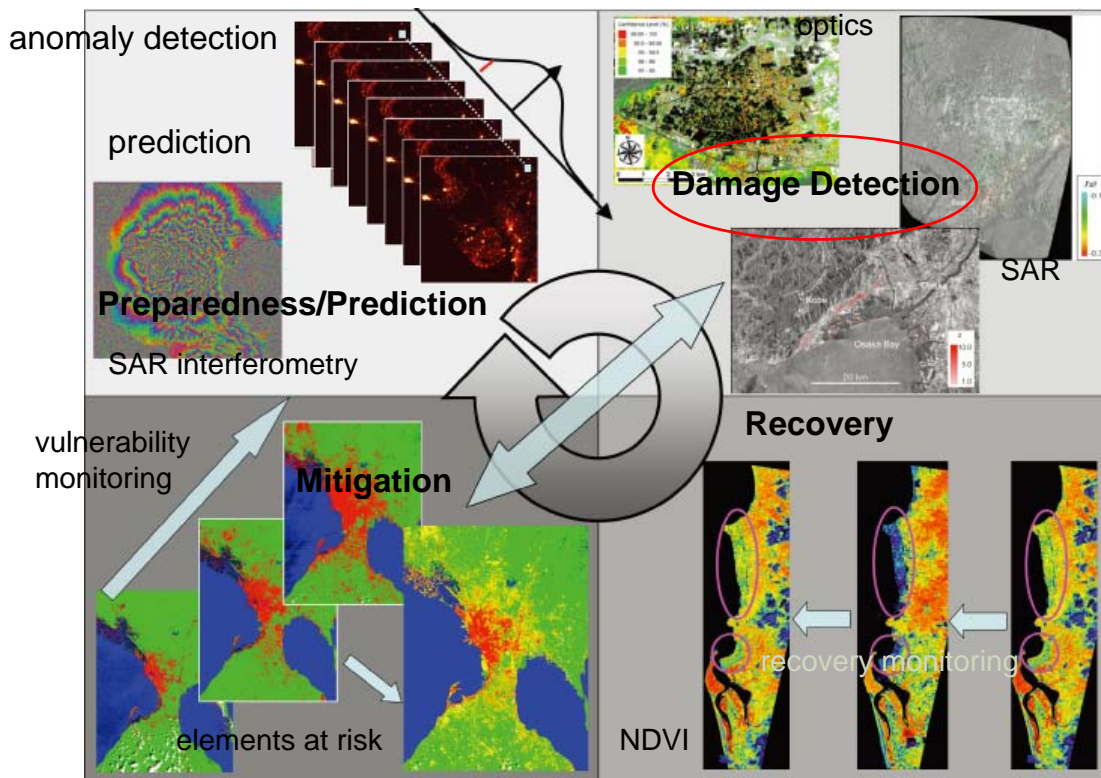
“Remote” means far away.  
Remote sensing means sensing things from a distance. Of **our** five senses **we** use three as remote sensors when we:

- watch a football game from the stands (sense of sight)
- smell freshly baked bread in the oven (sense of smell)
- hear a telephone ring (sense of hearing)

What are our other two senses and why aren't they used “remotely”?

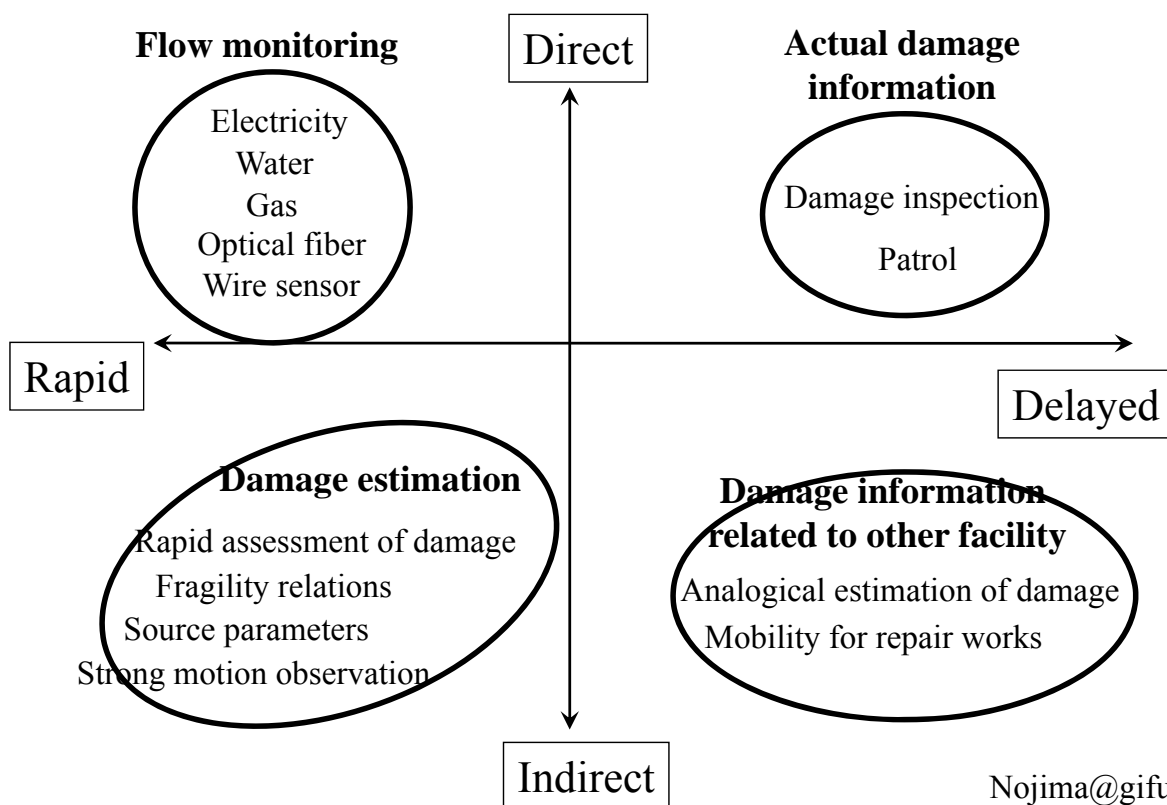
**five senses** [touch, taste, hearing, **eyesight**, and smell]<sub>2</sub>

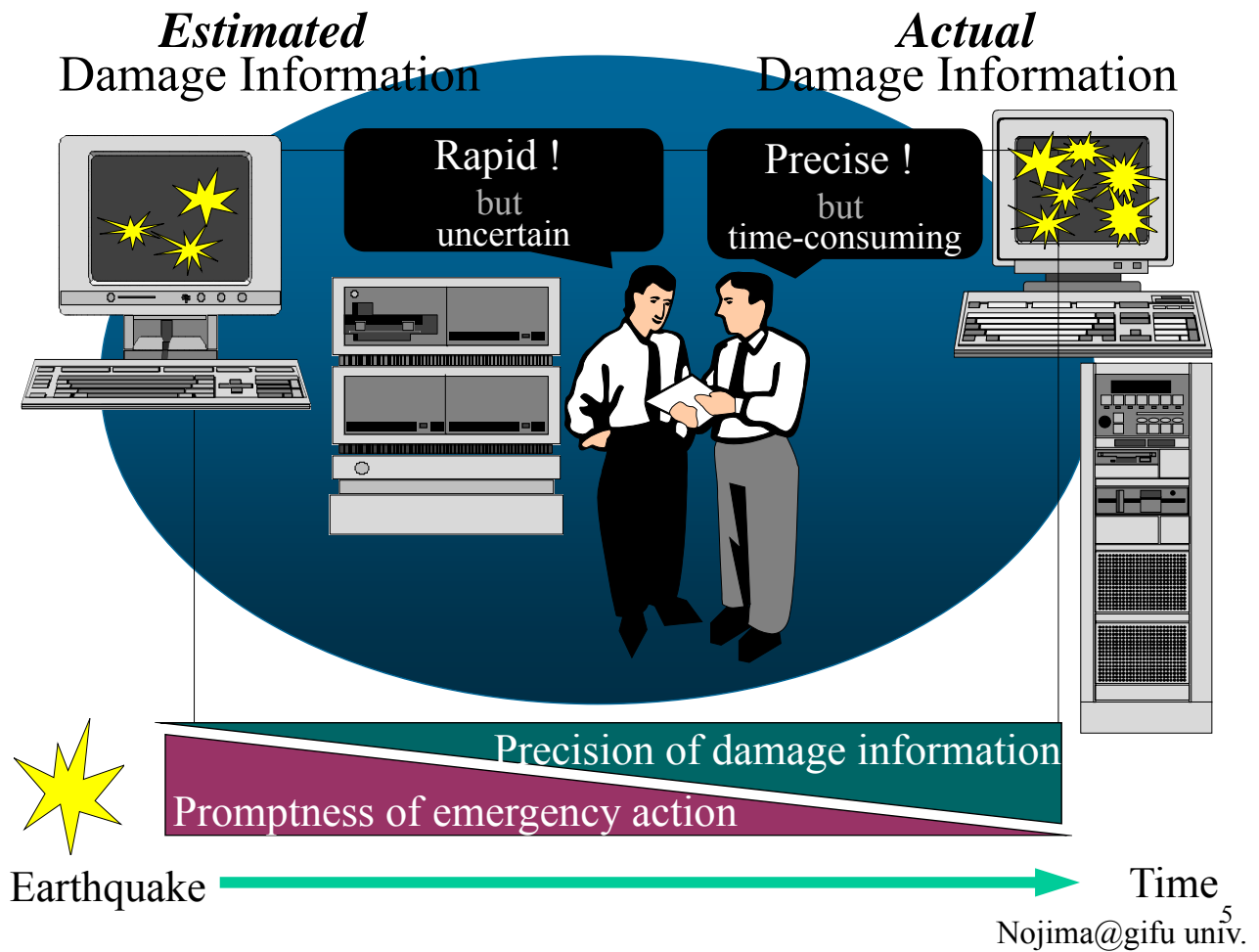
# Information from Remote Sensing data in terms of Disaster Management Cycle



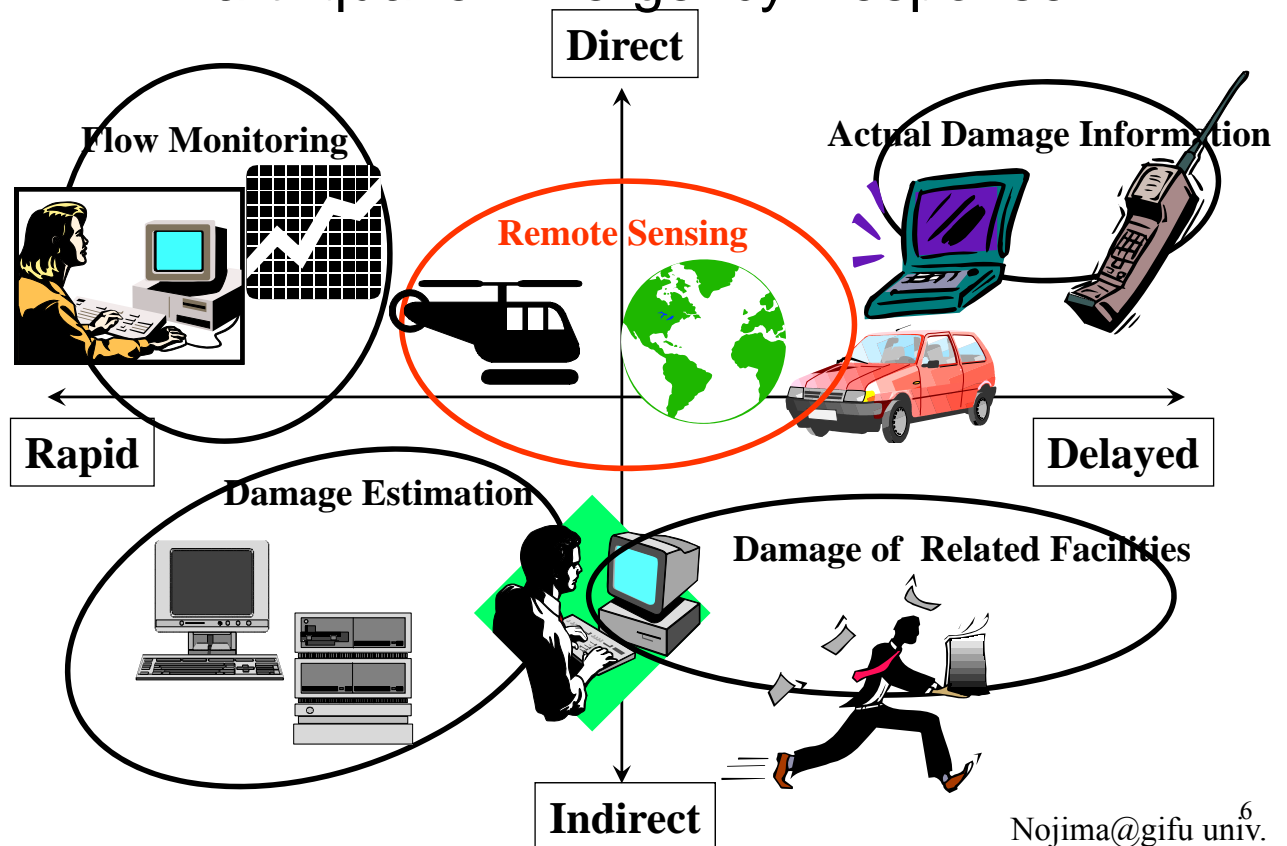
3

# Various Information Sources for Earthquake Emergency Response



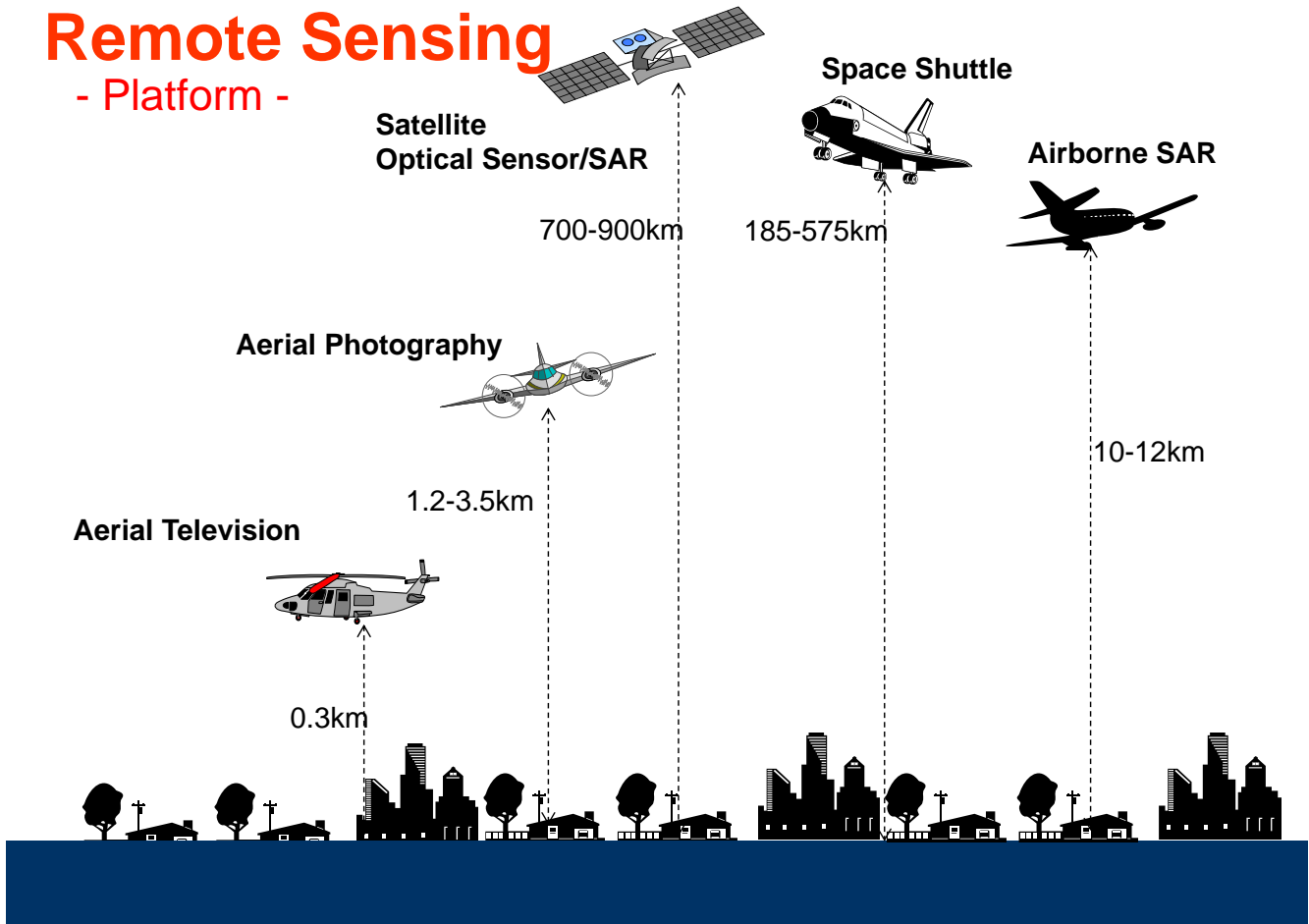


## Various Information Sources for Earthquake Emergency Response



# Remote Sensing

- Platform -



## Damage Assessment (Resolution-based Comparison)

- **Macro Scale Estimation**  
Meteorological Satellites  
(MTSAT, NOAA, DMSP, etc.)
- **Intermediate Scale Detection**  
Earth Observatory Satellites  
(ALOS, Landsat, SPOT, Envisat, etc.)
- **Micro Scale Identification**  
High-resolution Satellites,  
Airplane, Helicopter

# Spatial Resolution of Satellites

- Images where only large features are visible are said to have **coarse or low resolution**.
- In **fine or high resolution** images, small objects can be detected. **Military** sensors for example, are designed to view as much detail as possible, and therefore have very fine resolution.
- **Commercial** satellites provide imagery with resolutions **varying** from a few meters to several kilometers.
- Generally speaking, **the finer the resolution, the less total ground area** can be seen.



9

## Multispectral Sensors of Moderate-Resolution Satellites

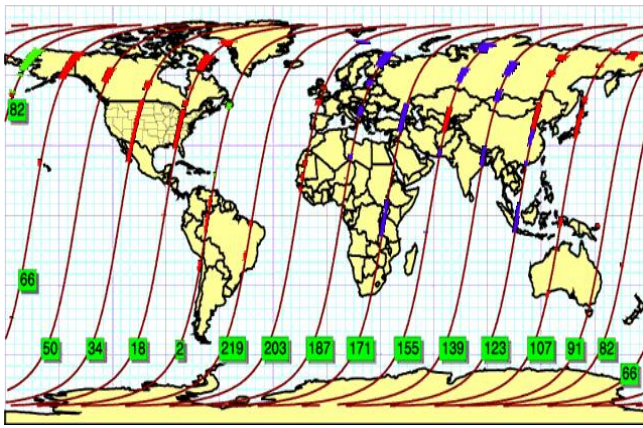
| Multispectral                     |                         |                              |                                |                                 |                    |   |   |                                  |
|-----------------------------------|-------------------------|------------------------------|--------------------------------|---------------------------------|--------------------|---|---|----------------------------------|
| Sensor - Satellite                |                         | Sponsor                      | Lifespan                       | Spatial Resolution              | Swath              | Spectral Bands  | Other Sensor Specs  | Repeat Cycle                     |
| <a href="#">Landsat 4 &amp; 5</a> | TM                      | NASA/NOAA/USGS               | 1984-                          | 30m MS<br>120m TIR              | 185x172 km         | MS 7 Bands VNIR-TIR   |   | 16 days                          |
| <a href="#">Landsat 7</a>         | ETM+                    | NASA/NOAA/USGS               | April 15th 1999 - ongoing**    | 15m Pan<br>30m MS<br>60m TIR    | 185x172 km         | Pan 520-900nm<br>5 Bands VNIR<br>2 Bands SWIR<br>1 Band TIR   | ** Data quality dropped significantly since the SLC failure in June 2003. | 16 days                          |
| <a href="#">SPOT 4</a>            | 2xHRV-IR & Vegetation   | <a href="#">CNES</a>         | March 1998 - ongoing ?         | 10m Pan<br>20m MS               | 60x60 km           | MS 4 bands (500-590, 610-680, 790-890, 1580-1750nm)<br>Pan (610-680nm)  | Also Vegetation Instrument at 1.1km pixel                                 | 3 to 26 days<br>±27° inclination |
| <a href="#">IRS-P6</a>            | LISS-4, LISS-3 & AWiFS  | <a href="#">INDIA (ISRO)</a> | Oct. 2003 - ongoing            | 5.8, 23.5 & 56m                 | 23.9, 141 & 740 km | LISS-4 3 bands 520-860nm  |   | 24 days                          |
| <a href="#">ASTER</a>             | <a href="#">Terra</a>   | MIT/NASA                     | December 1999<br>6 yrs mission | 15m VNIR<br>30m SWIR<br>90m TIR | 60 km x 60 km      | 3 bands VNIR 520-860nm,<br>6 bands SWIR 1600-2430nm,<br>5 bands TIR 8125-11650nm,<br>Bands for stereoscopy 780- | ASTER DEM product available, about 30m accuracy.                          | 16 days                          |
| <a href="#">CBERS-2</a>           | CCD Camera              | <a href="#">CHINA-BRAZIL</a> | Oct. 2003                      | 2 yrs                           | 20m                | CCD(high-res.,5bands)   | 113 km  | 26 days                          |
| <a href="#">ALOS</a>              | <a href="#">AVNIR-2</a> | <a href="#">JAXA</a>         | Jan. 2006                      | 10m MS                          |                    | 4 bands   |   | 46 days                          |
|                                   | <a href="#">PRISM</a>   | <a href="#">JAXA</a>         | Jan. 2006                      | 2.5m Pan                        |                    | 1 band  |   |                                  |

10

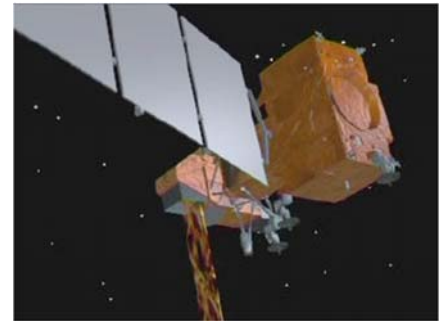


# Paths of Landsat 7

<http://landsat.usgs.gov/>



- = Path (orbit)
- = Path Number
- = USGS/EROS Data Center - Sioux Falls, SD
- = Svalbaard, Norway
- = Poker Flat, Alaska



Path and Row of Landsat 7 and the areas affected by the 2004 Indian Ocean Tsunami

11

## Sensors of High-Resolution Satellites

| High Resolution Sensor - Satellite | Sponsor                              | Lifespan                                | Spatial Resolutio                          | Swath   | Spectral Bands   | Other Sensor Specs                                       | Repeat Cycle                         |
|------------------------------------|--------------------------------------|---|--|---|--|--|--------------------------------------|
| ORBView-3                          | Orbimage                             | June 2003<br><br>5 yrs mission          | 1m Pan<br><br>4m MS                        | 8 km  | MS 4 bands (450-520, 520-600, 620-690, 760-900nm)<br>Pan (450-900nm)                                   | ±45° off nadir   | < 3 days                             |
| Quickbird-2                        | DigitalGlobe                         | Oct. 2001 - ongoing                     | 0.61m Pan<br><br>2.44m MS                  | 16.5 km<br><br>165 km track                       | MS 4 bands (450-520, 520-600, 630-690, 760-890nm)<br>Pan (450-900nm)                                   | QB 2 polar orbit<br><br>±30° in all directions<br>Stereo | 1-3.5 days                           |
| IKONOS-2                           | Space Imaging                        | Sept. 1999 - ongoing                    | 1m Pan<br><br>4m MS                        | 11.3 km wide at nadir                             | MS 4 bands (450-520, 520-600, 630-690, 760-900nm)<br>Pan (525.8-928.5nm)                               | ±26° inclination<br><br>11 bits data                     | 1-3 days                             |
| EROS 1A                            | West Indian                          | Dec. 2000 - ongoing                     | 1.8m Pan                                   | 12.6x12.6 km                                      | Pan (500-900nm)  |  | 1.8-4 days                           |
| SPOT 5a                            | HGR & Vegetation<br>Spot Image       | May 2002<br><br>> 5 yrs mission ?       | 2.5 & 5m Pan<br><br>10m MS<br><br>20m SWIR | 60 km   | MS 4 bands (500-590, 610-680, 790-890, 1580-<br>Pan 510-730nm  | Also Vegetation Instrument                               | 3 to 26 days<br><br>±31° inclination |
| IRS-1C & 1D                        | LISS3 & WiFS sensors<br>INDIA (ISRO) | 1C: Dec. 95 - ongoing<br>1D: Sept. 97 - | 5m Pan<br><br>20m MS<br><br>180m WiFS      | 70x70 km Pan<br>142x142 km MSS<br>774x774 km WiFS | Pan 500-750nm<br><br>MS 4 bands (520-590, 620-680, 770-860, 1550-<br>WiFS 2 bands (620-680, 770-860nm) | Pan ±26° inclination                                     | 24 days<br><br>5-24 off-nadir Pan    |

|             |              |             |          |            |                                |  |          |
|-------------|--------------|-------------|----------|------------|--------------------------------|--|----------|
| WorldView-1 | DigitalGlobe | Sept. 2007  | 0.5m Pan | 17.6km Pan |                                |  | 1.7 days |
| WorldView-2 | DigitalGlobe | Oct.. 2009  | 0.5m Pan | 16.4km     | MS 8 bands (1.8m) + Pan (0.5m) |  | 1.1 days |
| GeoEye-2    | GeoEye       | Sept.. 2008 | 0.4m Pan | 15.2km     | MS bands (1.6m) + Pan (0.4m)   |  | 2.1 days |

# QuickBird-2

## Launch

on October 18, 2001

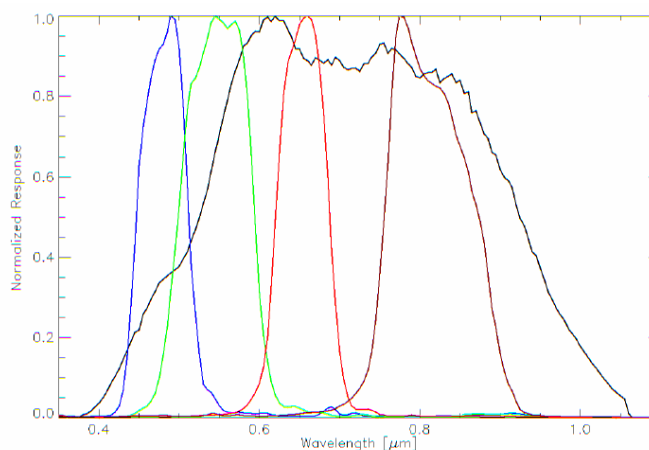
## Features

Highest resolution sensors commercially available

## Sensor Resolution

61-cm panchromatic at nadir  
2.44-m multi-spectral at nadir

|                       |                   |
|-----------------------|-------------------|
| <b>Blue -Band 1</b>   | <b>450-520 nm</b> |
| <b>Green -Band 2</b>  | <b>520-600 nm</b> |
| <b>Red -Band 3</b>    | <b>630-690 nm</b> |
| <b>Near IR-Band 4</b> | <b>760-900 nm</b> |
| <b>Panchromatic</b>   | <b>450-900 nm</b> |

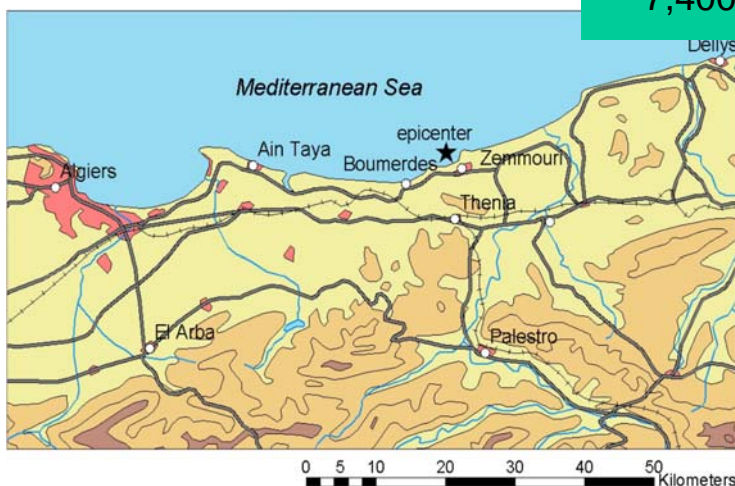


Normalized QB spectral band responses

13  
<http://www.digitalglobe.com>

## QuickBird Captured Affected Areas of the 2003 Boumerdes, Algeria Earthquake

- Mw = 6.8
- The epicenter is located offshore of the province of Boumerdes.
- Approximate numbers of collapsed and heavily damaged buildings were 7,400 and 7,000, respectively.





# South Campus, Boumerdes University

C



Photo by Dr. K. Meguro on 22 July, 2003

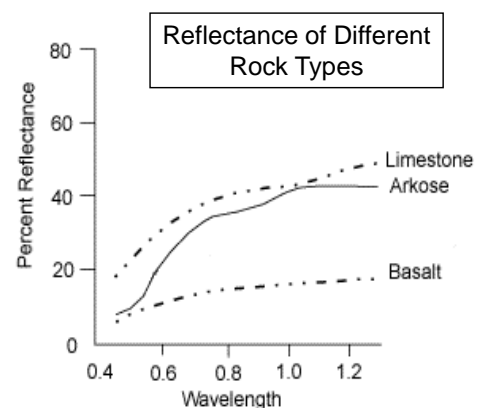
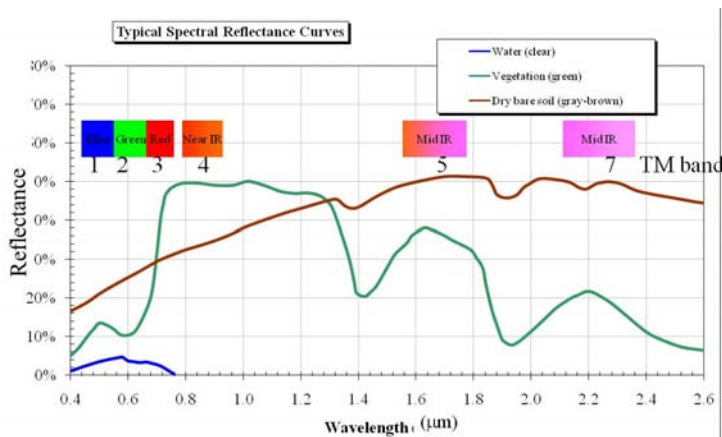


15

## Spectral Resolution

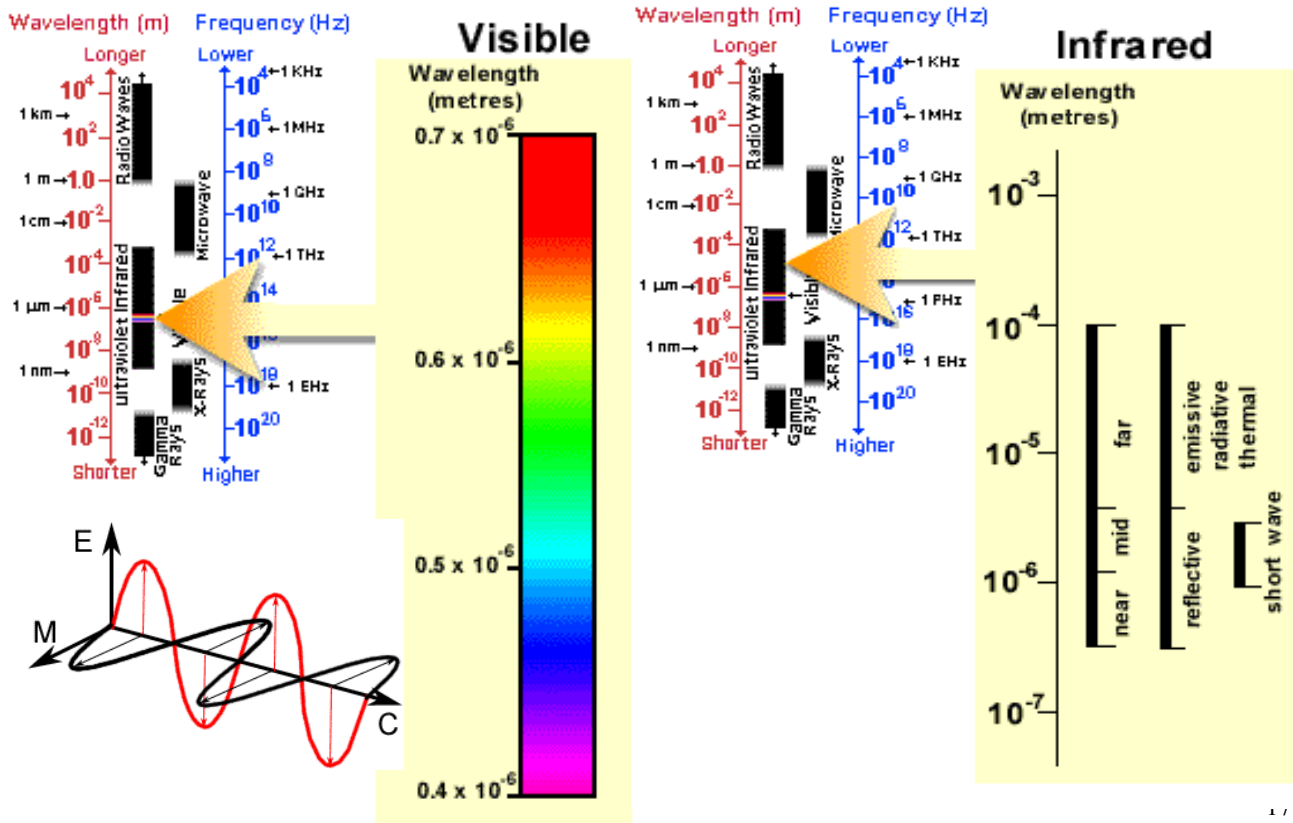
Different classes of features and details in an image can often be distinguished by comparing their responses over distinct wavelength ranges. **Broad classes**, such as water and vegetation, can usually be separated **using very broad wavelength ranges** - the visible and near infrared .

Other **more specific classes**, such as different rock types, may not be easily distinguishable using these broad wavelength ranges and would require comparison **at much finer wavelength ranges** to separate them.



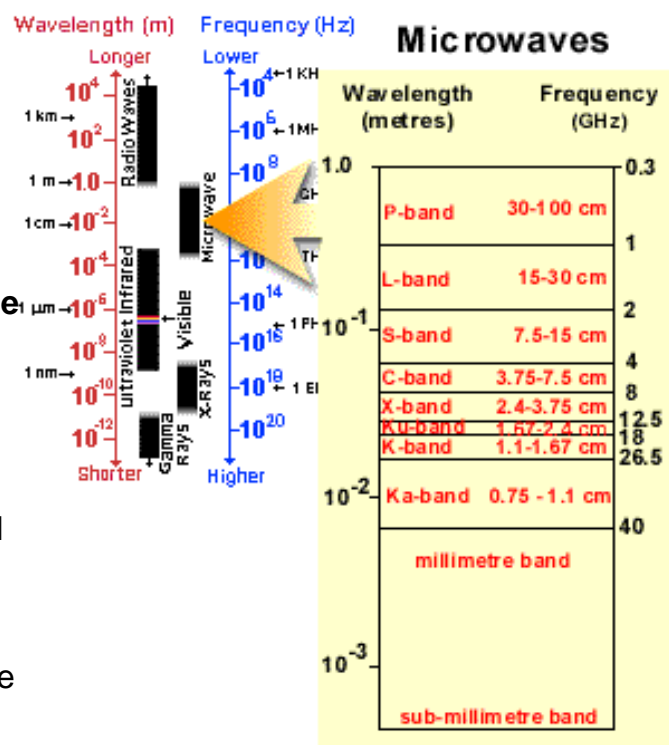


# Electromagnetic Spectrum



## Microwave fundamentals

- **Ka, K, and Ku bands:** very short wavelengths used in early airborne radar systems but uncommon today.
- **X-band:** used extensively on airborne systems (e.g. PI-SAR) for military reconnaissance and terrain mapping.
- **C-band:** common on many airborne research systems (e.g. NASA AirSAR) and spaceborne systems (ERS-1, 2 and RADARSAT).
- **S-band:** used on board the Russian ALMAZ satellite.
- **L-band:** used onboard SEASAT and JERS-1 satellites and airborne systems.
- **P-band:** longest radar wavelengths, used on NASA experimental airborne research system.

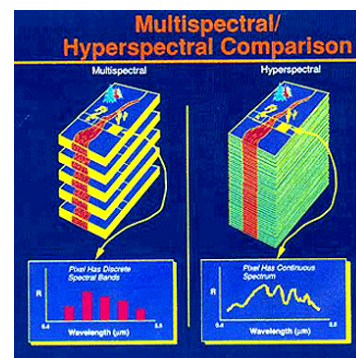


# Multi-spectral and Hyper-spectral Sensors

Many remote sensing systems record energy over **several separate wavelength** ranges at various spectral resolutions. These are referred to as **multi-spectral sensors**.

Advanced multi-spectral sensors called **hyperspectral** sensors, detect **hundreds of very narrow spectral bands** throughout the **visible, near-IR, and mid-IR** portions of the EM spectrum.

Their very high spectral resolution facilitates **fine discrimination** between different targets based on their spectral response in each of the narrow bands.



19

## Hyperspectral Sensors

| Hyperspectral             |                          |  |   |                                 |                 |  |                                       |         |
|---------------------------|--------------------------|--|---|---------------------------------|-----------------|--|---------------------------------------|---------|
| Sensor - Satellite        | Sponsor                  | Lifespan                                 | Spatial Resolution  | Swath                           | Spectral Bands  | Other Sensor Specs   | Repeat Cycle                          |         |
| <a href="#">EO-1</a>      | <a href="#">Hyperion</a> | <a href="#">NASA</a>                     | Dec. 1999 - ongoing !<br><br>(sept. 2003)<br>1 yr mission | 30m                             | 7.5 km x 100 km | 220 bands 400nm to 2500nm @10nm<br>Grating Imaging Spec<br><br>Grating Imaging Spec  |                                       |         |
| <a href="#">EO-1</a>      | <a href="#">LEISA AC</a> | <a href="#">NASA</a>                     | 12/1/1999<br>1 yr mission                                 | 250m                            | 7.5 km x 100 km | 309 Bands 850-1600nm @2.4nm<br>Wedge Imaging Spec  |                                       |         |
| <a href="#">Envisat-1</a> | <a href="#">MERIS</a>    | ESA<br>Aerospatiale France, Cannes, ACRI | May 2002<br>5 yrs mission                                 | 300m<br>@nadir and 1200m global | 1150 km         | 15 bands programmable<br>390-1040nm @2.5nm   | 5 identical sensors                   | 35 days |
| <a href="#">ADEOS-2</a>   | GLI                      | NASDA                                    | Dec. 2002 - Oct. 2003<br>3 yrs design                     | 250/1000m                       |                 | 19 bands 375-865nm @8-20nm<br>4 bands 460-825nm @50-110nm<br>6 bands 1050-2210nm @20-220nm<br>7 bands 3715-12000nm @330-1000nm | Failed prematurely on october 25 2003 |         |

# Terra-MODIS (Moderate Resolution Imaging Spectroradiometer)

Sees every point on our world every **1-2 days**  
in **36 discrete spectral bands**.



| Primary Use                               | Band | Bandwidth    |
|---|------|--------------|
| Land/Cloud Boundaries                     | 1    | 620- 670     |
| Land/Cloud Properties                     | 2    | 841- 876     |
| Land/Cloud Properties                     | 3    | 459- 479     |
| Land/Cloud Properties                     | 4    | 545- 565     |
| Land/Cloud Properties                     | 5    | 1230- 1250   |
| Land/Cloud Properties                     | 6    | 1628- 1652   |
| Land/Cloud Properties                     | 7    | 2105- 2155   |
| Ocean Color/Phytoplankton/Biogeochemistry | 8    | 405- 420     |
| Ocean Color/Phytoplankton/Biogeochemistry | 9    | 438- 448     |
| Ocean Color/Phytoplankton/Biogeochemistry | 10   | 483- 493     |
| Ocean Color/Phytoplankton/Biogeochemistry | 11   | 526- 536     |
| Ocean Color/Phytoplankton/Biogeochemistry | 12   | 546- 556     |
| Ocean Color/Phytoplankton/Biogeochemistry | 13   | 662- 672     |
| Ocean Color/Phytoplankton/Biogeochemistry | 14   | 673- 683     |
| Ocean Color/Phytoplankton/Biogeochemistry | 15   | 743- 753     |
| Ocean Color/Phytoplankton/Biogeochemistry | 16   | 862- 877     |
| Atmospheric                               | 17   | 890- 920     |
| Water Vapor                               | 18   | 931- 941     |
| Water Vapor                               | 19   | 915- 965     |
| Surface/Cloud                             | 20   | 3.660- 3.840 |

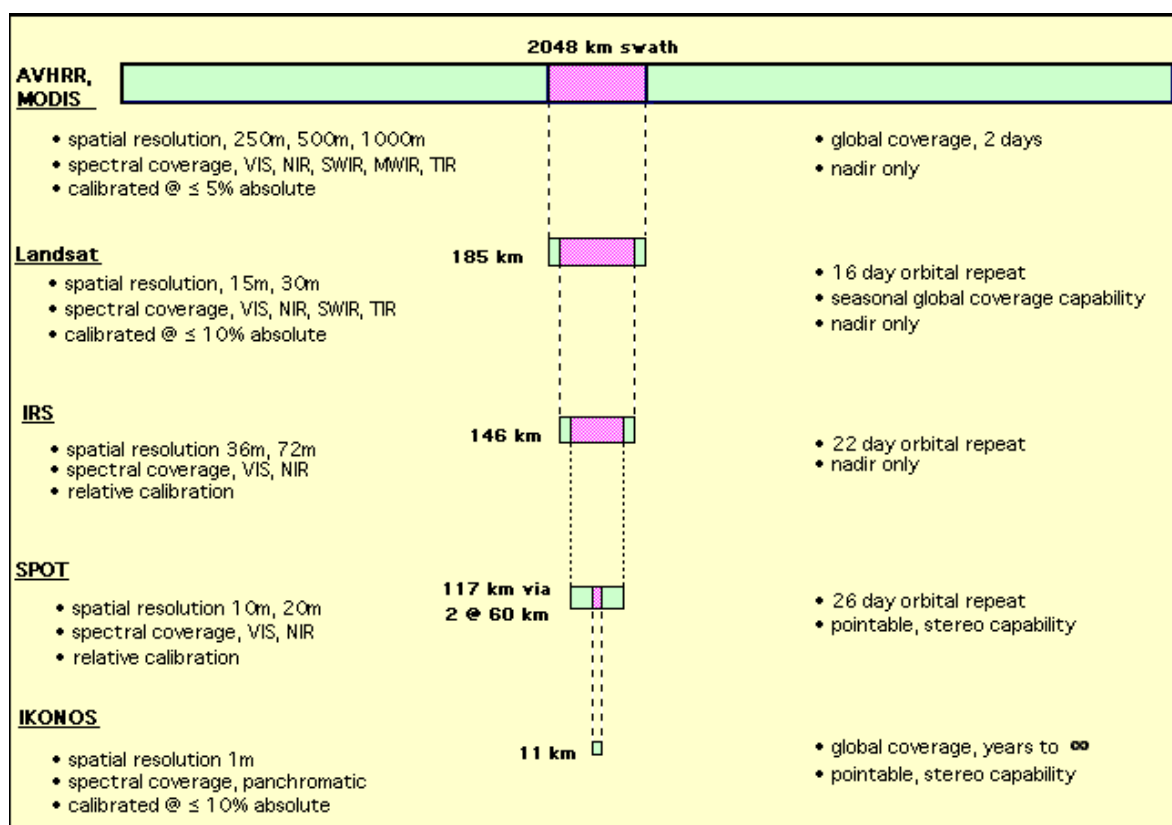
|               |    |                |
|---------------|----|----------------|
| Temperature   | 21 | 3.929- 3.989   |
| Temperature   | 22 | 3.929- 3.989   |
| Temperature   | 23 | 4.020- 4.080   |
| Atmospheric   | 24 | 4.433- 4.498   |
| Temperature   | 25 | 4.482- 4.549   |
| Cirrus Clouds | 26 | 1.360- 1.390   |
| Water Vapor   | 27 | 6.535- 6.895   |
| Water Vapor   | 28 | 7.175- 7.475   |
| Water Vapor   | 29 | 8.400- 8.700   |
| Ozone         | 30 | 9.580- 9.880   |
| Surface/Cloud | 31 | 10.780- 11.280 |
| Temperature   | 32 | 11.770- 12.270 |
| Cloud Top     | 33 | 13.185- 13.485 |
| Altitude      | 34 | 13.485- 13.785 |
| Altitude      | 35 | 13.785- 14.085 |
| Altitude      | 36 | 14.085- 14.385 |

Bands 1 to 19, nm; Bands 20-36,  $\mu\text{m}$   
Spatial Resolution: 250 m (bands 1-2)  
(at nadir): 500 m (bands 3-7)  
1000 m (bands 8-36)



21

## Swath of various satellites



22

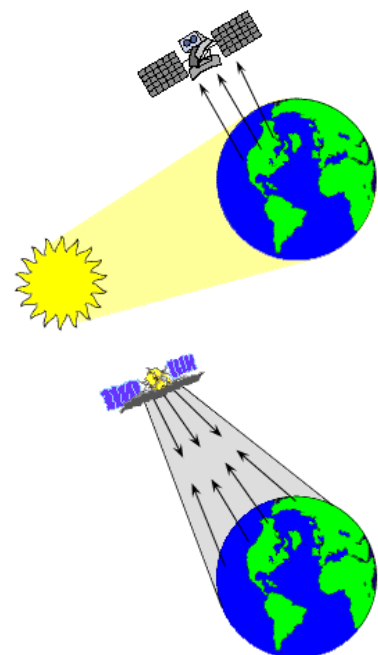
# Type of Sensors

- ✓ Optical
  - ✓ Visible and near-infrared
  - ✓ Thermal
- ✓ LiDAR (Light Detection And Ranging)
- ✓ Radar (Radio Detection And Ranging)

23

## The Remote Sensing Framework

- Source of Energy
  - Passive Sources (Natural)
    - Reflected solar radiation
    - Emitted terrestrial radiation
  - Active Sources (Man-made)
    - Flash photography
    - Radar/LIDAR/Sonar



24



# International Charter on Space and Major Disasters

- Background
  - Following the UNISPACE III conference held in Vienna, Austria in July 1999, the European and French space agencies (ESA and CNES) initiated the [International Charter “Space and Major Disasters”](#), with the Canadian Space Agency (CSA) signing the Charter on October 20, 2000. In September of 2001, the National Oceanic and Atmospheric Administration (NOAA) and the Indian Space Research Organization (ISRO) also became members of the Charter. The Argentine Space Agency (CONAE) joined in July 2003. The Japan Aerospace Exploration Agency (JAXA) became a member in February 2005. The United States Geological Survey (USGS) has also joined the Charter as part of the U.S. team. BNSC/DMC and China National Space Administration (CNSA) became a member in November 2005 and May 2007, respectively.
- Aim and activity
  - The International Charter aims at providing a unified system of space data acquisition and delivery to those affected by natural or man-made disasters through authorized users. Each member agency has committed resources to support the provisions of the Charter and thus is helping to mitigate the effects of disasters on human life and property.
  - Earth Observation (EO) satellite image-based maps and other regional maps are also opened to public through the web site. (<http://www.disasterscharter.org/>)

25

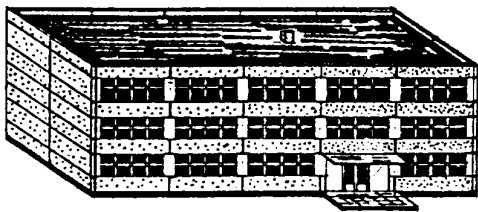
## Index in Building Damage

Based on the classification of damage to buildings of reinforced concrete used in the European Macroseismic Scale (EMS)

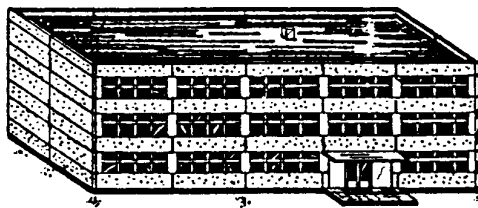
| Index   | Description      | Interpretation  |
|---------|------------------|---|
| Grade 1 | Slight Damage    | Cosmetic cracking, no observable distress to load bearing structural elements           |
| Grade 2 | Moderate Damage  | Cracking in load bearing elements, but no significant displacements across the cracks   |
| Grade 3 | Heavy Damage     | Cracking in load bearing elements with significant deformations across the cracks       |
| Grade 4 | Partial Collapse | Collapse of portion of the building in plan view (i.e. a corner, or a wing of building) |
| Grade 5 | Collapse         | Collapse of the complete structure or loss of a floor of the structure                  |

26

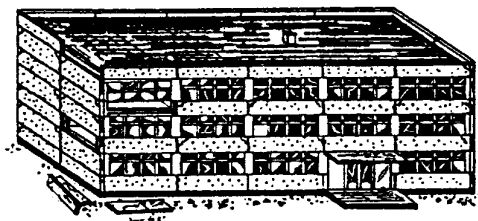
# Classification of damage to buildings of reinforced concrete used in the European Macroseismic Scale (EMS)



**Grade 1: Negligible to slight damage**  
**(no structural damage, slight non-structural damage)**  
Fine cracks in plaster over frame members or in walls at the base.  
Fine cracks in partitions and infills.



**Grade 2: Moderate damage**  
**(slight structural damage, moderate non-structural damage)**  
Cracks in columns and beams of frames and in structural walls.  
Cracks in partition and infill walls; fall of brittle cladding and plaster.  
Falling mortar from the joints of wall panels.

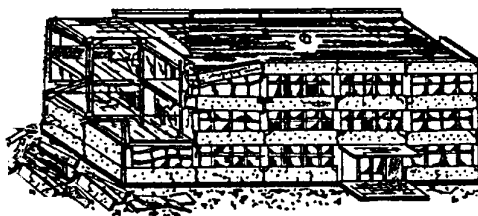


**Grade 3: Substantial to heavy damage**  
**(moderate structural damage, heavy non-structural damage)**  
Cracks in columns and beam column joints of frames at the base and at joints of coupled walls. Spalling of concrete cover, buckling of reinforced rods.  
Large cracks in partition and infill walls, failure of individual infill panels.

[http://www.gfz-potsdam.de/portal/gfz/Struktur/Departments/Department+2/sec26/projects/04\\_seismic\\_vulnerability\\_scales\\_risk/EMS-](http://www.gfz-potsdam.de/portal/gfz/Struktur/Departments/Department+2/sec26/projects/04_seismic_vulnerability_scales_risk/EMS-)

27

# Classification of damage to buildings of reinforced concrete used in the European Macroseismic Scale (EMS)



**Grade 4: Very heavy damage (heavy structural damage, very heavy non-structural damage)**  
Large cracks in structural elements with compression failure of concrete and fracture of rebars; bond failure of beam reinforced bars; tilting of columns. Collapse of a few columns or of a single upper floor.

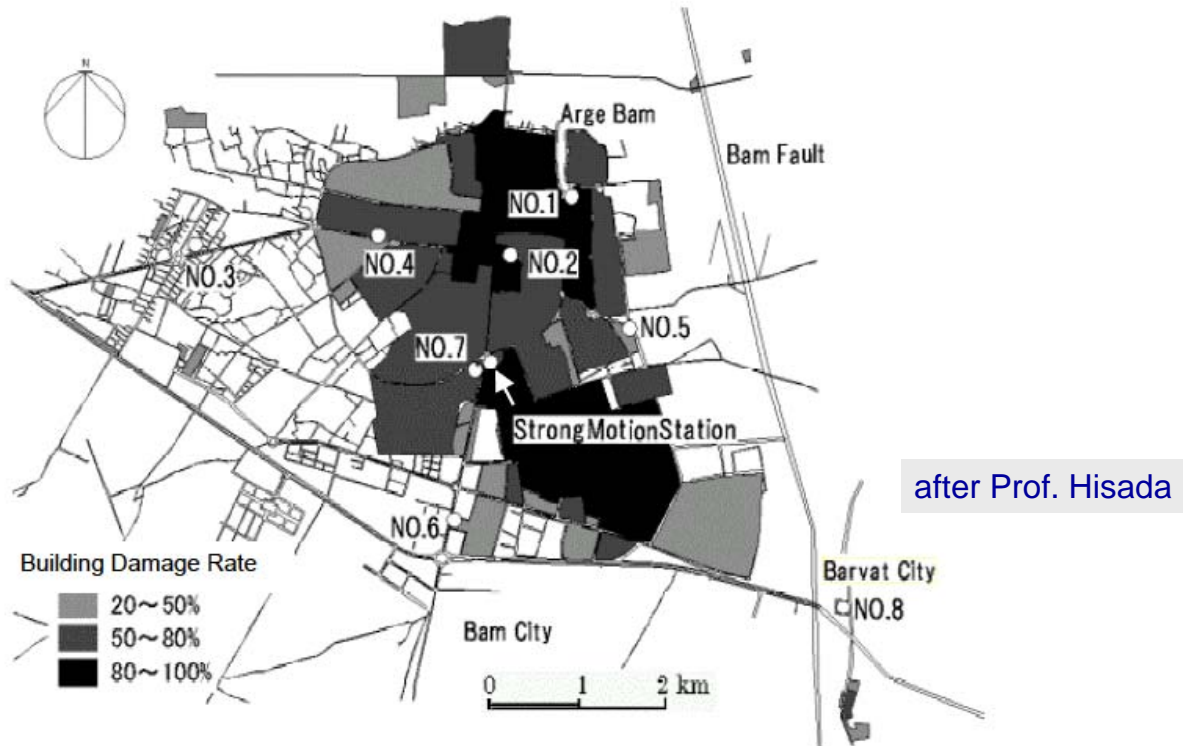


**Grade 5: Destruction**  
**(very heavy structural damage)**  
Collapse of ground floor or parts (e. g. wings) of buildings.

[http://www.gfz-potsdam.de/portal/gfz/Struktur/Departments/Department+2/sec26/projects/04\\_seismic\\_vulnerability\\_scales\\_risk/EMS-](http://www.gfz-potsdam.de/portal/gfz/Struktur/Departments/Department+2/sec26/projects/04_seismic_vulnerability_scales_risk/EMS-)

28

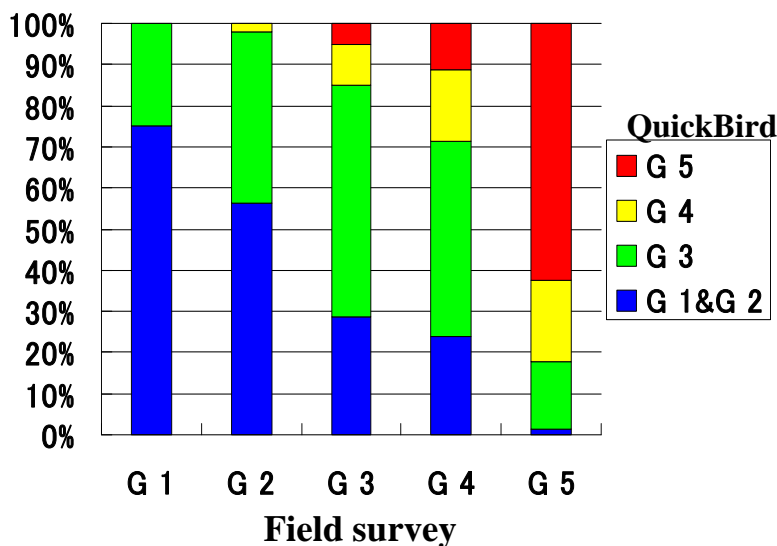
# Damage map of Bam and Baravat and the strong motion and aftershock stations



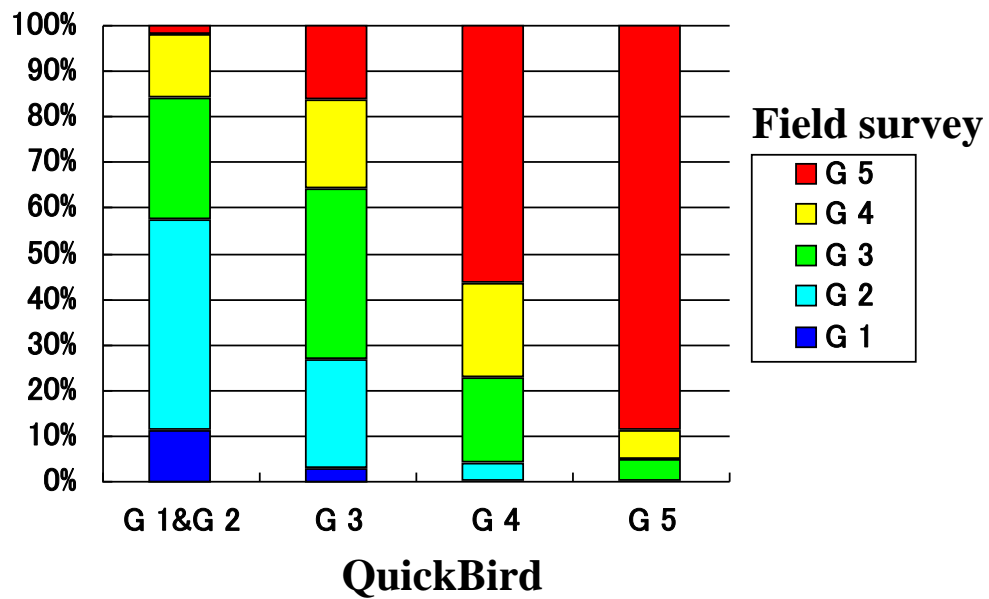
29

## Summary of comparison for 7 stations

| Field survey \ QuickBird | G 1 | G 2 | G 3 | G 4 | G 5 | sum |
|--------------------------|-----|-----|-----|-----|-----|-----|
| G 1 & G 2                | 12  | 50  | 29  | 15  | 2   | 108 |
| G 3                      | 4   | 37  | 57  | 30  | 25  | 153 |
| G 4                      | 0   | 2   | 10  | 11  | 30  | 53  |
| G 5                      | 0   | 0   | 10  | 7   | 95  | 107 |
| sum                      | 16  | 89  | 101 | 63  | 152 | 421 |



# Summary of comparison for 7 stations



31

## Damage Detection

- Visual Interpretation
- Image Processing
  - Color composite (pre- and post-event)
  - Index (band ratio, texture...)
  - Supervised Classification
  - Non-supervised Classification

32



# High-resolution Satellite Images Before and After Tsunami

- Banda Aceh: QuickBird, res.: ps.0.6m, swath: 40km -

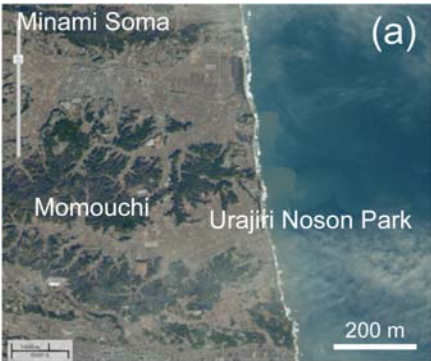
Pre-tsunami image (June 23, 2004)

Post-tsunami image (Dec. 29, 2004)

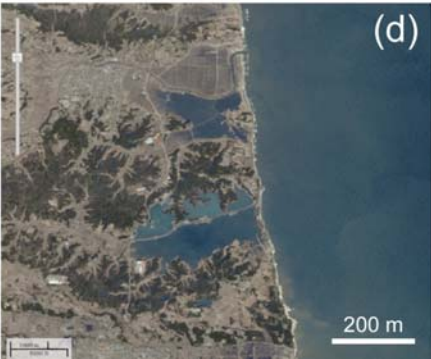
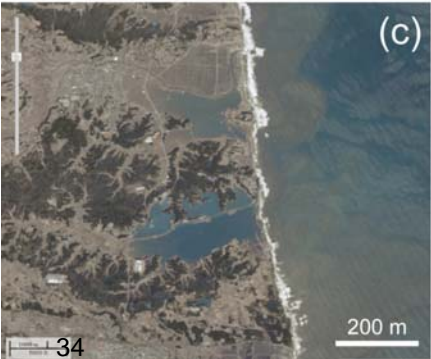


33  
source: UNOSAT

# ASTER Images Before and After Tsunami

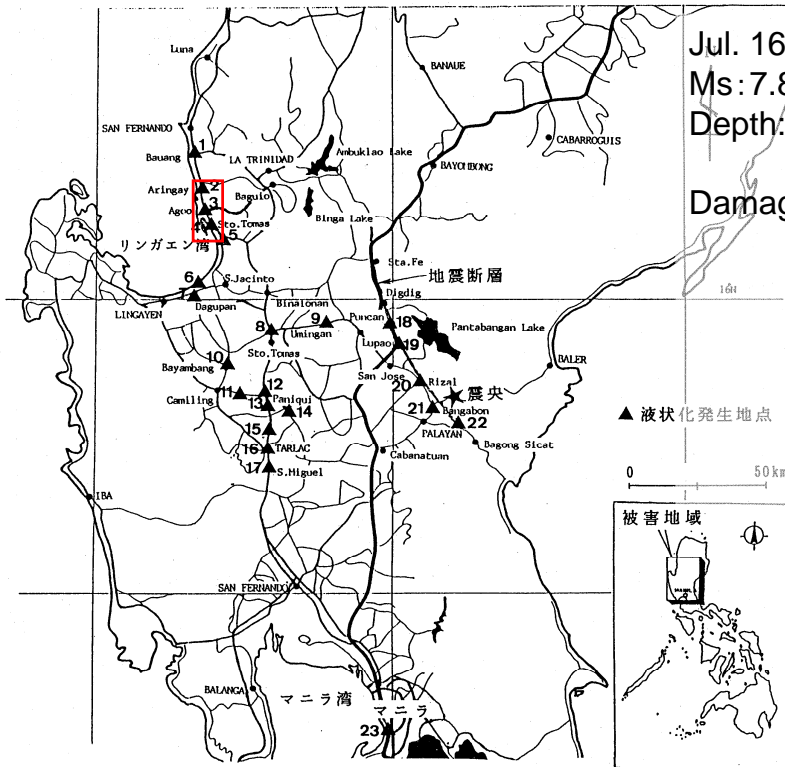


- (a) 2008/12/25
- (b) 2011/3/14
- (c) 2011/3/19
- (d) 2011/3/28



Minami-Soma  
Considerable erosion and remaining water, even two weeks after the earthquake

# The 1990 Luzon Earthquake, The Philippines



Jul. 16, 1990  
 Ms: 7.8, Mw: 7.6  
 Depth: 25km

Damage (Aug. 12, 1990)  
 death toll: 1,666  
 missing: 460  
 injured: 3,516  
 severe and moderate damage:  
 104,614 buildings  
 damage cost: 99 billion Peso  
 (400 billion yen, US\$ 3 billion)

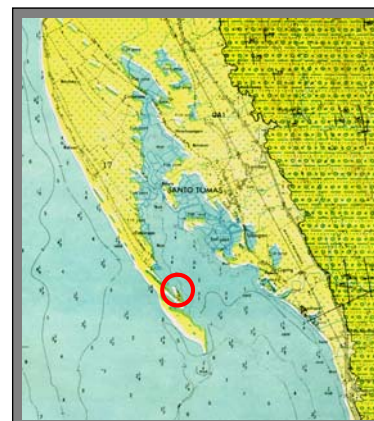
## Damage at East Coast of Lingayen Gulf



図4.1 リンガエン湾東部沿岸地域における液状化発生日点

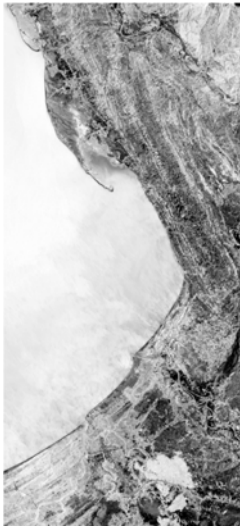


Barrio Narvacan  
 (villages sunk into the sea due to liquefaction)





# Color Composite Image to Estimate Damaged Areas



Inverse image of post-event (for red color)

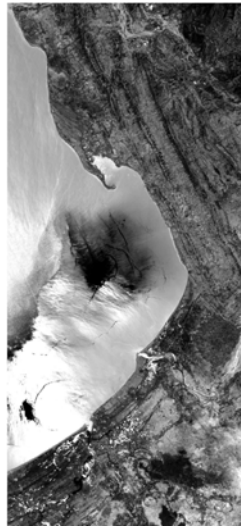
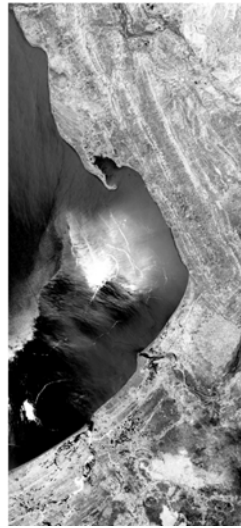
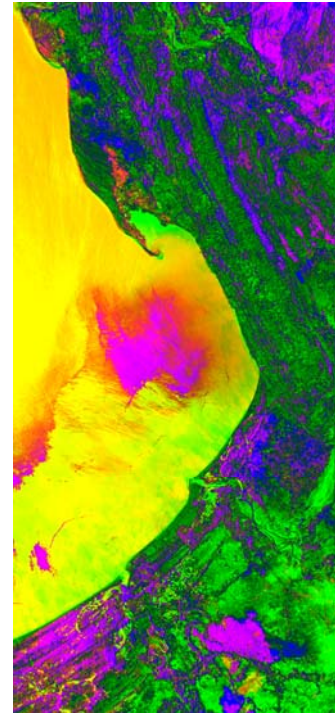


Image of pre-event (for green color)

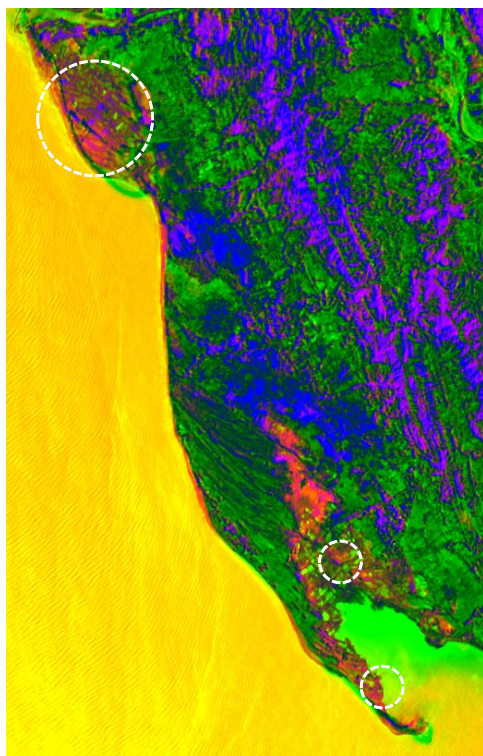


Inverse image of pre-event (for blue color)



Pink color area  
...reflectance became low (area of sunk into the sea due to EQ.)<sup>37</sup>

# Comparison with Survey Report



Color composite image

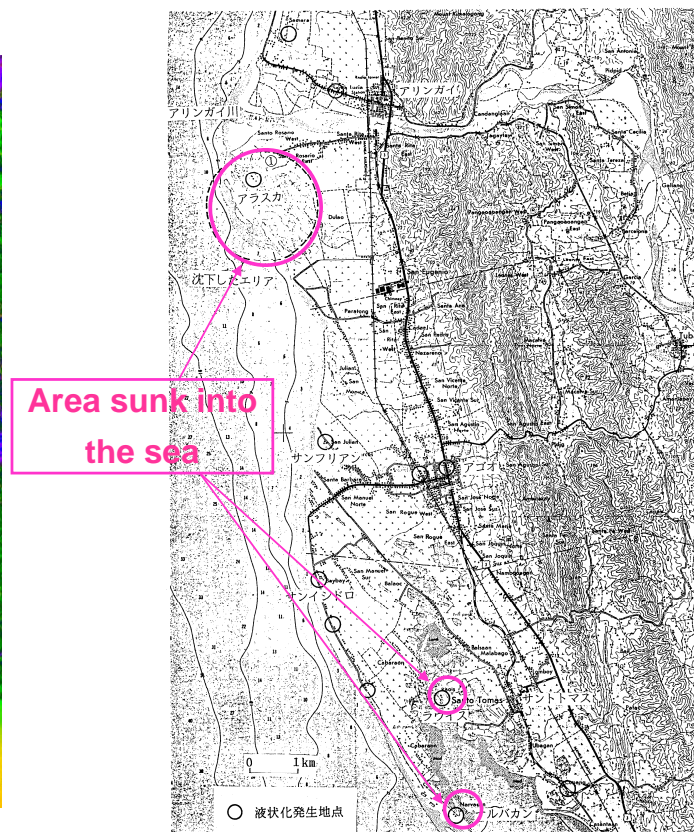


図4.1 リンガエン湾東部沿岸地域における液状化発生日点



# Tsunami-Affected Area Detection

Sumatra Earthquake Tsunami on Dec. 23, 2004

ASTER (15 m resolution)



**KHAO LAK,  
Phang nga,  
THAILAND**

Easily to detect the boundary of the affected areas because vegetation was stripped away.



2002/11/15



2004/12/31<sup>39</sup>

© METI and NASA

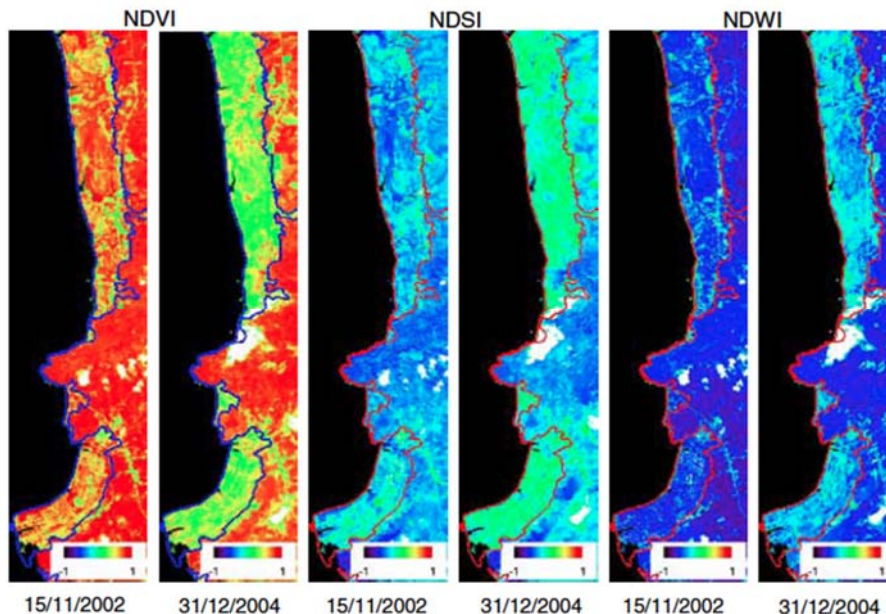
## Several Indices of Tsunami Damaged Area

ASTER (15 m resolution)

Normalized Difference Vegetation Index,  $NDVI = (NIR - Red) / (NIR + Red)$

Normalized Difference Soil Index,  $NDSI = (SWIR - NIR) / (SWIR + NIR)$

Normalized Difference Water Index,  $NDWI = (Red - SWIR) / (Red + SWIR)$



Yamazaki et al., Forecast of Tsunamis from the Japan-Kuril-Kamchatka Source Region, Natural Hazards, Volume 38, Number 3, July 2006, pp. 411-435(25) Springer, DOI: <http://dx.doi.org/10.1007/s11069-005-2075-7>



# Automated Damage Detection Technique Using Image Texture

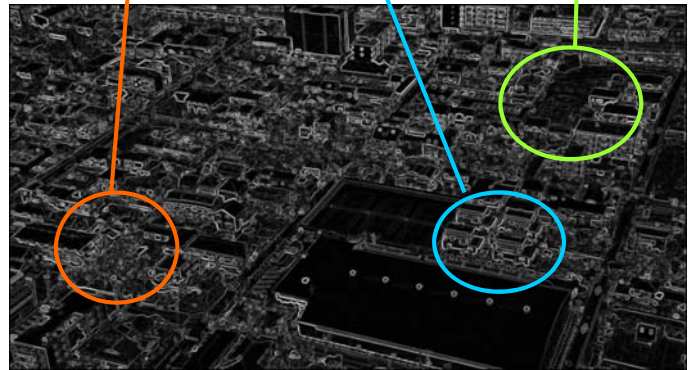
Jan. 27, 1995  
(10 days after the Kobe EQ )  
HDTV (High definition TV)

9 cm/pixel (lower)  
17 cm/pixel (upper)



Nishinomiya City  
HDTV image taken on 1995/1/27

Edge intensity image



## Procedure of Edge-based Damage Detection

- Edge textures are computed from the intensity image
- Edge intensity ( $E_i$ ) is maximum value in eight directions derived from  $7 \times 7$  Prewitt filter.
- Using  $E_i$ , edge intensity variance ( $E_v$ ) is computed in  $7 \times 7$  local window.
- The ratio of predominant direction of  $E_i$  ( $E_d$ ) is also computed in  $7 \times 7$  local window.
- Then, co-occurrence textures: angular second moment ( $T_a$ ) and entropy ( $T_e$ ) are computed in  $7 \times 7$  local window.
- Collapsed buildings show a strong trend of non-uniformity. Our investigation showed the following threshold values are suitable,

Fig.10.9.1 Examples of spatial filters of  $3 \times 3$  window

| SPATIAL FILTERS          | $3 \times 3$ OPERATOR   | EFFECTS                          |
|--------------------------|---|----------------------------------|
| <b>Sobel</b>             | $ A  +  B $ or $\sqrt{A^2+B^2}$ where,<br>$A = \begin{bmatrix} -1 & 0 & 1 \\ -2 & 0 & 2 \\ -1 & 0 & 1 \end{bmatrix}$ $B = \begin{bmatrix} -1 & -2 & -1 \\ 0 & 0 & 0 \\ 1 & 2 & 1 \end{bmatrix}$ | gradient<br>(finite differences) |
| <b>Gradient -Prewitt</b> | $ A  +  B $ or $\sqrt{A^2+B^2}$ where,<br>$A = \begin{bmatrix} -1 & 0 & 1 \\ -1 & 0 & 1 \\ -1 & 0 & 1 \end{bmatrix}$ $B = \begin{bmatrix} -1 & -1 & -1 \\ 0 & 0 & 0 \\ 1 & 1 & 1 \end{bmatrix}$ | gradient<br>(finite differences) |
| <b>Laplacian</b>         | $\begin{bmatrix} 0 & -1 & 0 \\ -1 & 4 & -1 \\ 0 & -1 & 0 \end{bmatrix}$ or $\begin{bmatrix} -1 & -1 & -1 \\ -1 & 8 & -1 \\ -1 & -1 & -1 \end{bmatrix}$  | differential                     |
| <b>smoothing</b>         | $\begin{bmatrix} 1/9 & 1/9 & 1/9 \\ 1/9 & 1/9 & 1/9 \\ 1/9 & 1/9 & 1/9 \end{bmatrix}$ or $\begin{bmatrix} 0 & 1/5 & 0 \\ 1/5 & 1/5 & 1/5 \\ 0 & 1/5 & 0 \end{bmatrix}$                          | smoothing                        |
| <b>median</b>            | Replaced with median of $3 \times 3$ window   | noise removal                    |
| <b>High-pass</b>         | $\begin{bmatrix} 0 & -1 & 0 \\ -1 & 5 & -1 \\ 0 & -1 & 0 \end{bmatrix}$ or $\begin{bmatrix} -1/9 & -1/9 & -1/9 \\ -1/9 & 8/9 & -1/9 \\ -1/9 & -1/9 & -1/9 \end{bmatrix}$                        | edge-enhancement                 |
| <b>sharpening</b>        | $\begin{bmatrix} 1/9 & -8/9 & 1/9 \\ -8/9 & 37/9 & -8/9 \\ 1/9 & -8/9 & 1/9 \end{bmatrix}$  | clear image                      |

## Edge Information (1)

### ■ Variance of edge intensity (7x7 pixel window)

“Collapsed” : a lot of edge elements

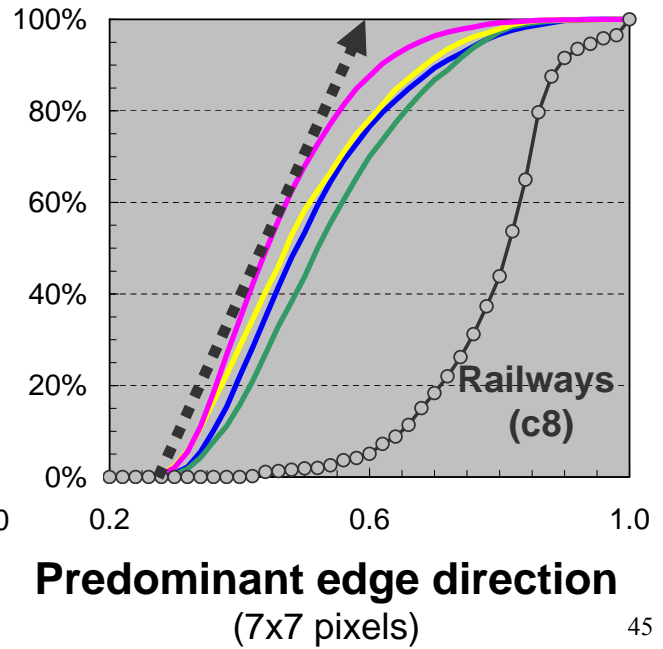
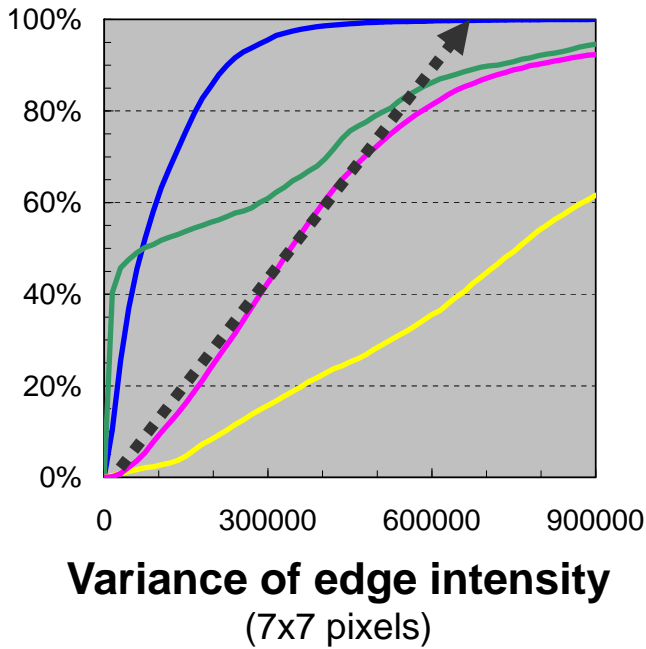
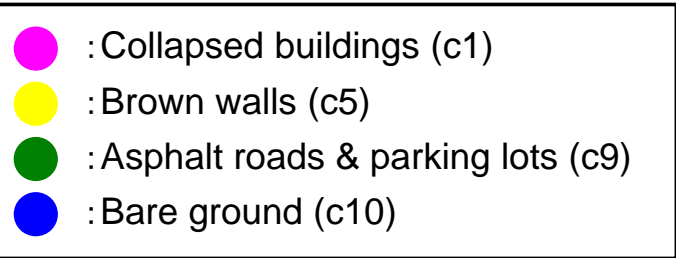
“Non-damaged” : a small of edge elements

### ■ Ratio of predominant edge direction (7x7 pixel window)

To distinguish between “Collapsed” and “Non-damaged”

[ Prewitt-type template can indicate an edge  
direction with the strongest edge intensity ]

## Cumulative Relative Frequencies for Training Data



45

## Edge Information (2)

### ■ Angular second moment (7x7 pixel window)

$$Ta = \sum_{k=0}^{15} \sum_{l=0}^{15} [\delta(k, l)]^2$$

large  $Ta$   $\longrightarrow$  uniform texture

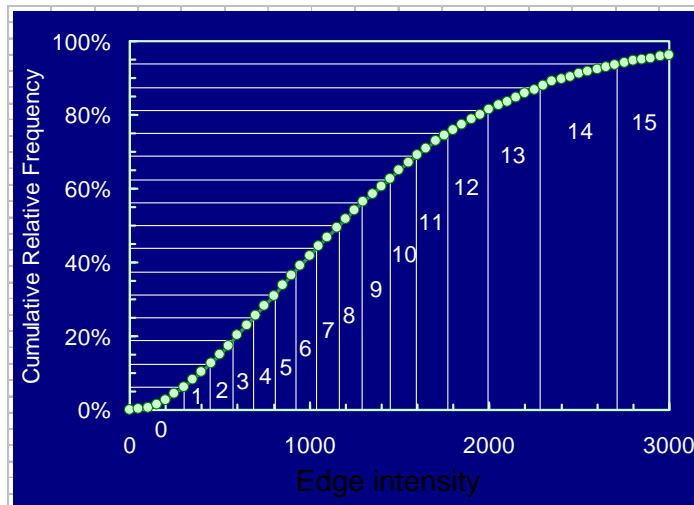
### ■ Entropy (7x7 pixel window)

$$Te = - \sum_{k=0}^{15} \sum_{l=0}^{15} [\delta(k, l) \log_e \delta(k, l)]$$

small  $Te$   $\longrightarrow$  uniform texture

46

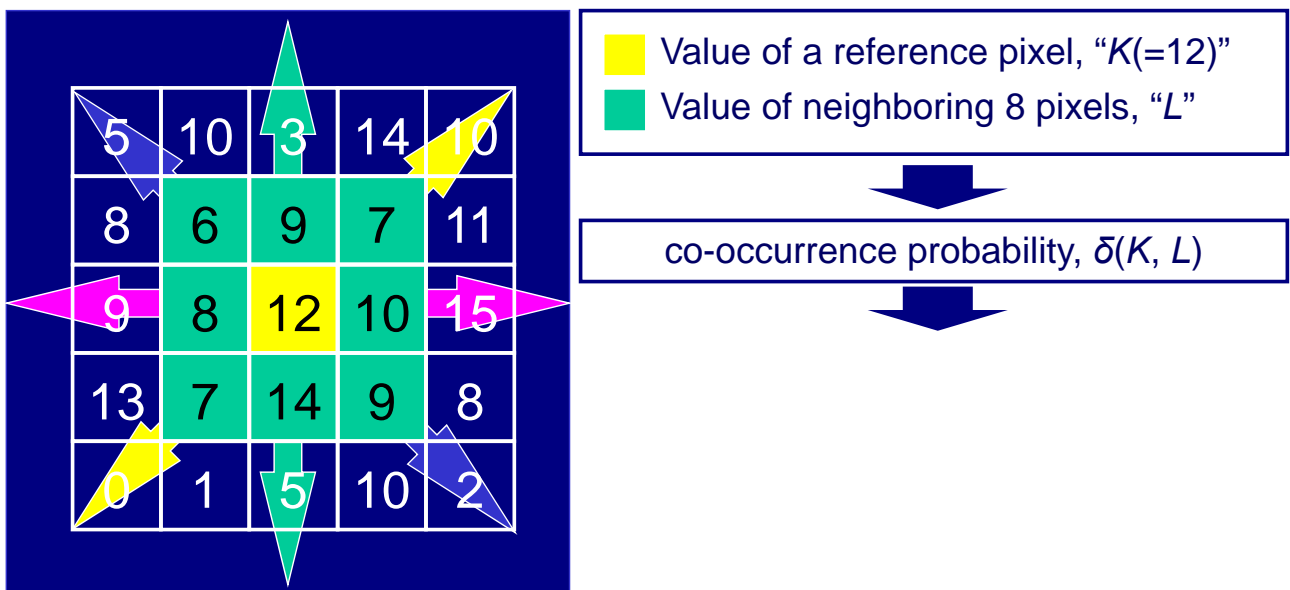
# How to derive “Edge Texture”



- Cumulative relative frequency of collapsed buildings (c1) is converted from 8 to 4-bit data

47

# How to derive “Edge Texture”

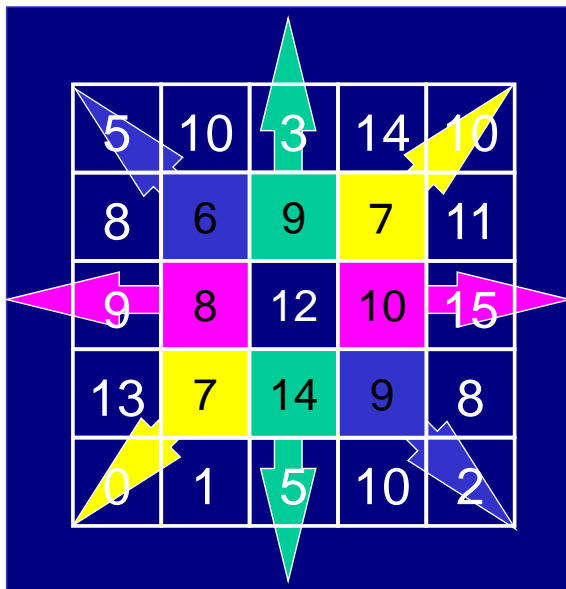


Edge intensity with 4-bit data

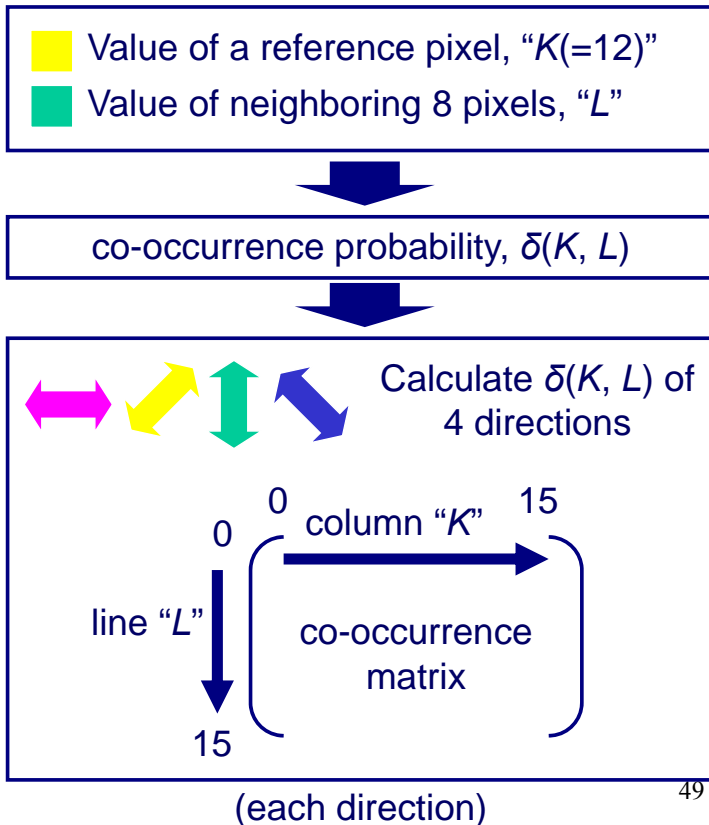
48



# How to derive “Edge Texture”



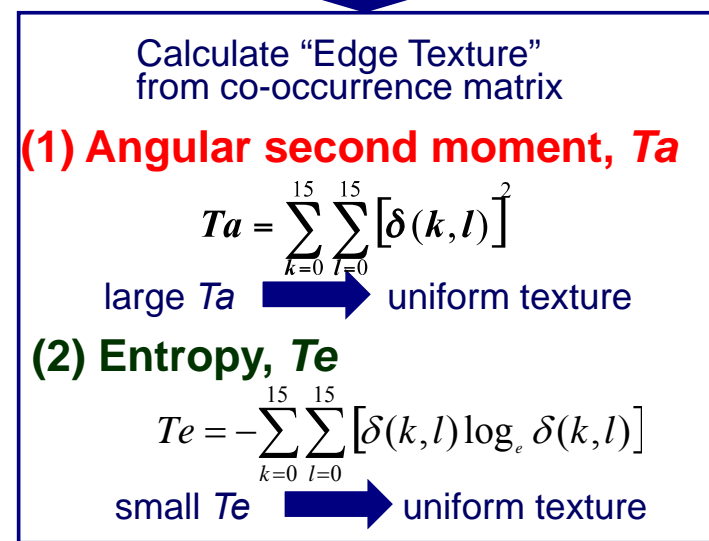
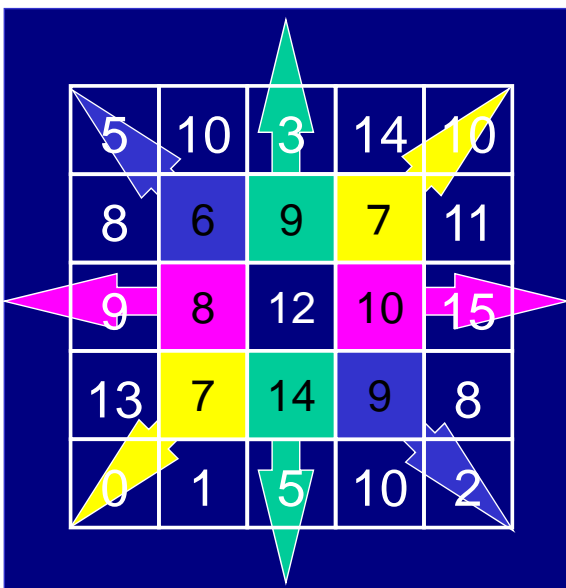
Edge intensity with 4-bit data



49

# How to derive “Edge Texture”

(each direction)

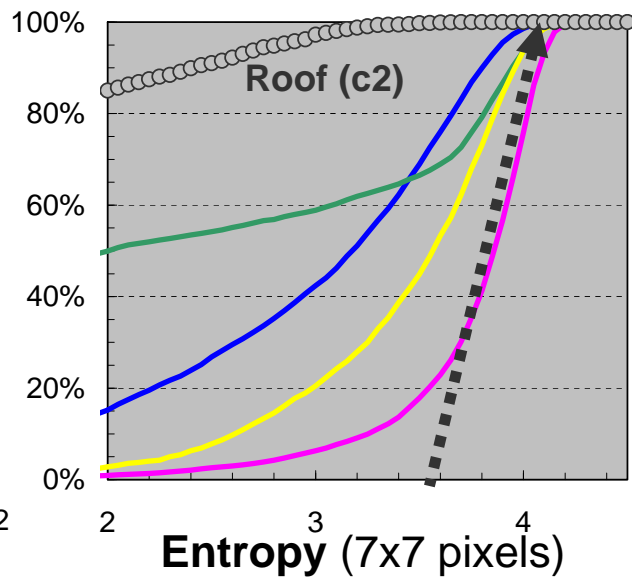
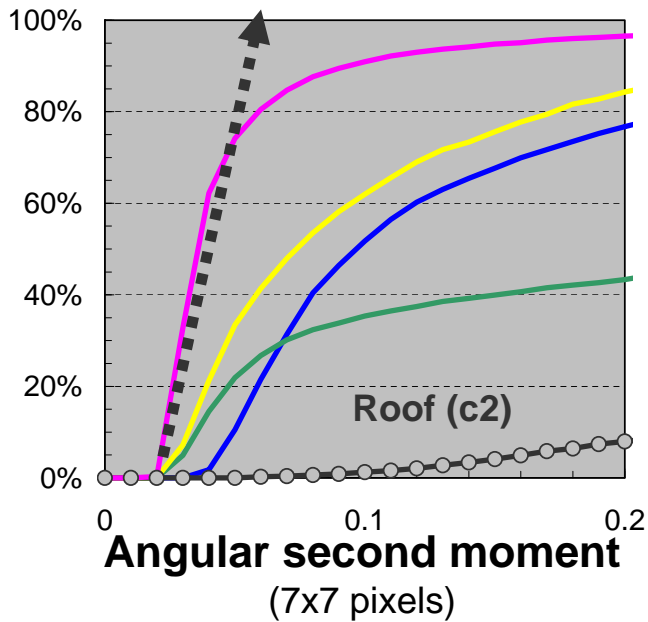
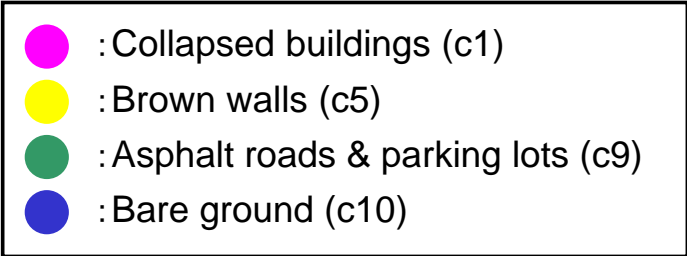


Representative texture value is . . .

Maximum value of textures derived from co-occurrence matrices in 4 directions

50

# Cumulative Relative Frequencies for Training Data



**Collapsed buildings show the strongest trends of non-uniformity**<sup>51</sup>

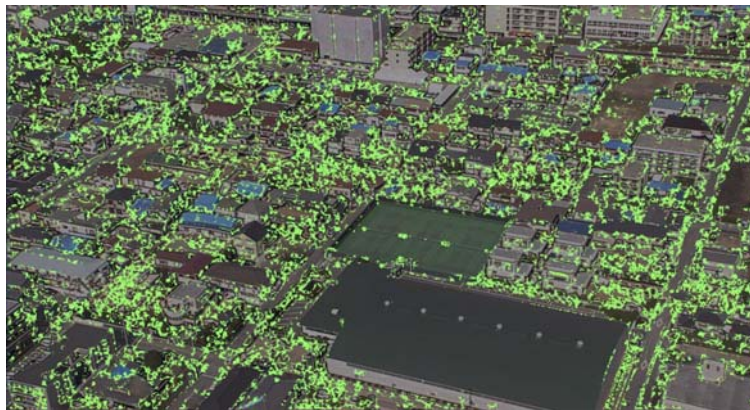
## Procedure of Edge-based Damage Detection

| Index                             | Threshold values                |
|-----------------------------------|---------------------------------|
| <i>Ev</i> (edge variance)         | 2.0 - 6.8 ( $\times 10^5$ )     |
| <i>Ed</i> (edge direction)        | 0.3 - 0.6                       |
| <i>Ta</i> (angular second moment) | 0.75 - 6.6 ( $\times 10^{-2}$ ) |
| <i>Te</i> (entropy)               | 3.5 - 4.2                       |

- Finally, local density of the detected pixels is assessed to remove the meaningless spots.

# Threshold Values to Extract Pixels in Damaged Areas

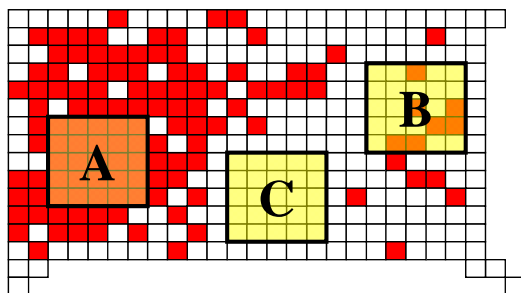
- Variance of edge intensity,  $E_v$ : 2.0 - 6.8 ( $\times 10^5$ )
- Predominant edge direction,  $E_d$ : 0.3 - 0.6
- Angular second moment,  $T_a$ : 0.75 - 6.6 ( $\times 10^{-2}$ )
- Entropy,  $T_e$ : 3.5 - 4.2



53

## Spatial Filtering

Calculate the percentage of the extracted pixels in the window of the size of approximately one building.




Example

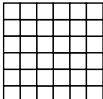
A : 1.00  
B : 0.24  
C : 0.00

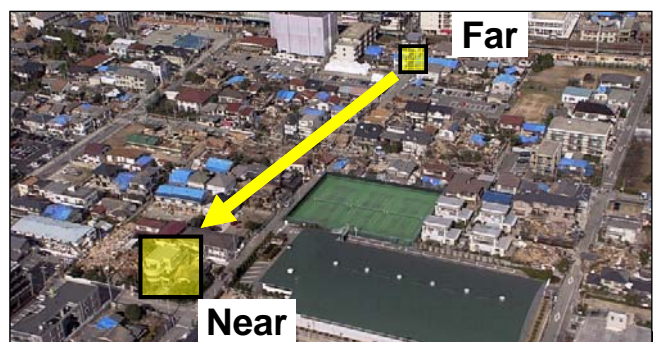
Red : the extracted pixels

Consider the influence of the distance from the camera

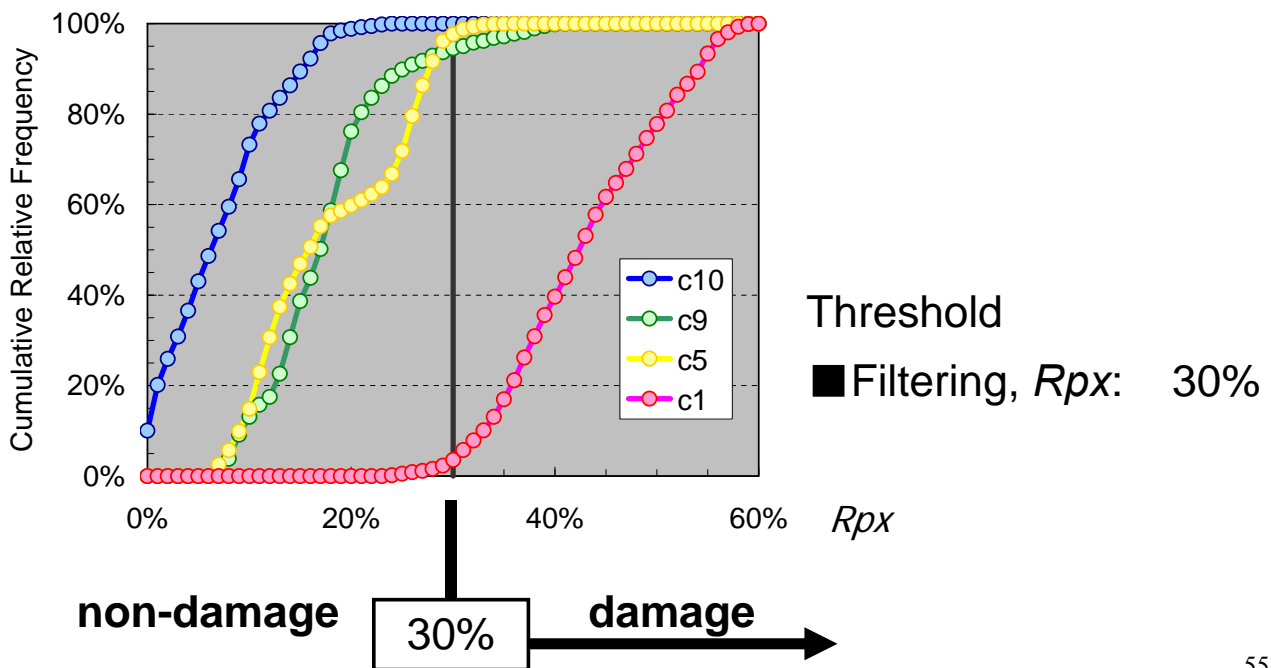
Far  31 x 31 pixels window

↓ Change a window width

Near  63 x 63 pixels window



# Cumulative Relative Frequency of Local Density of Extracted Pixels



55

## Result from Aerial Television Image taken after Kobe Earthquake

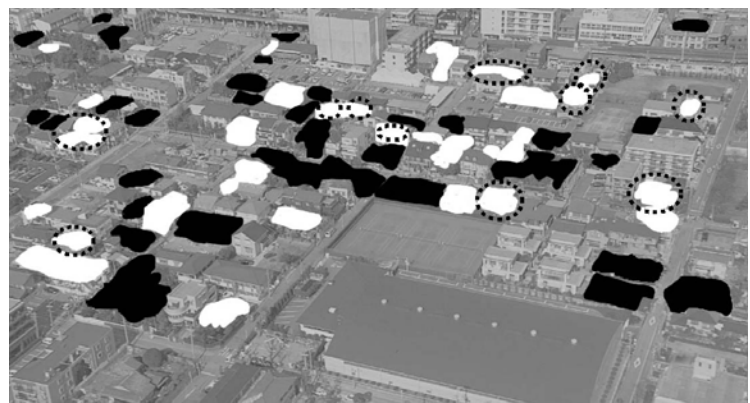


Estimated damage

Black: damaged building  
(level slice by edge  
information)

Actual damage by field survey

Black: collapsed  
 White: severe damage  
 (dotted area: plastic sheet  
 covered on roof)





# Near Real-time Damage Detection Using Only Post-event Aerial Images



## Application to Other Earthquakes



Aerial image of Golcuk, Turkey  
taken after the 1999 earthquake



Estimated damage



Black: damaged building  
Threshold values are same as the  
Kobe earthquake





# Application to Other Earthquakes



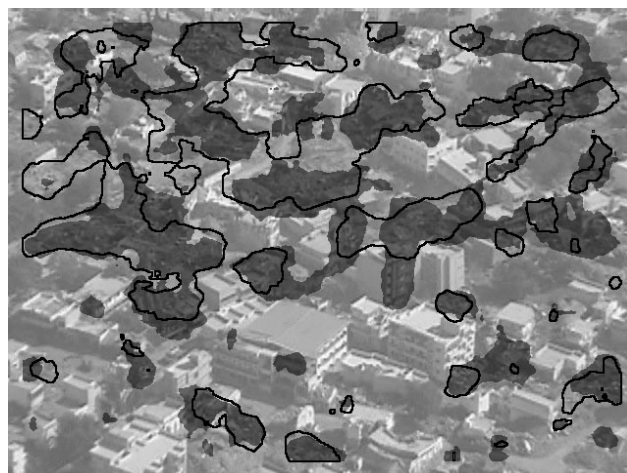
Aerial image of Bachau, India taken after the 2001 earthquake



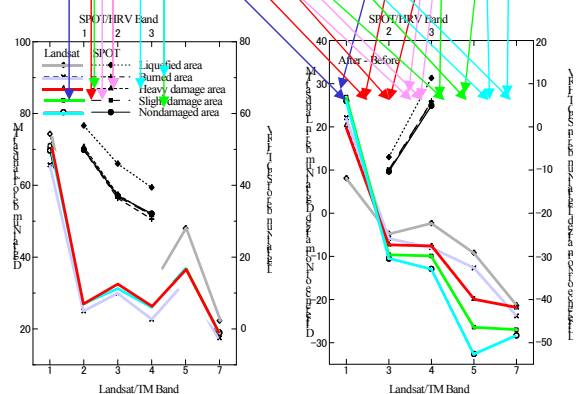
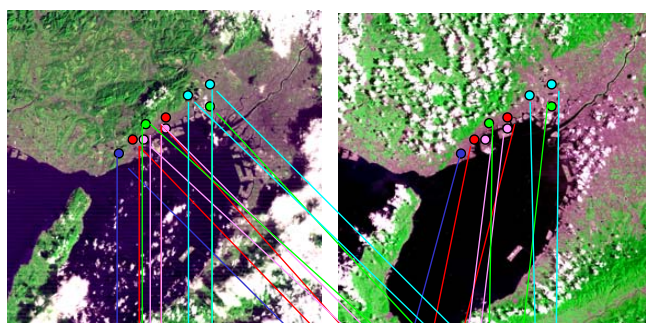
Estimated damage



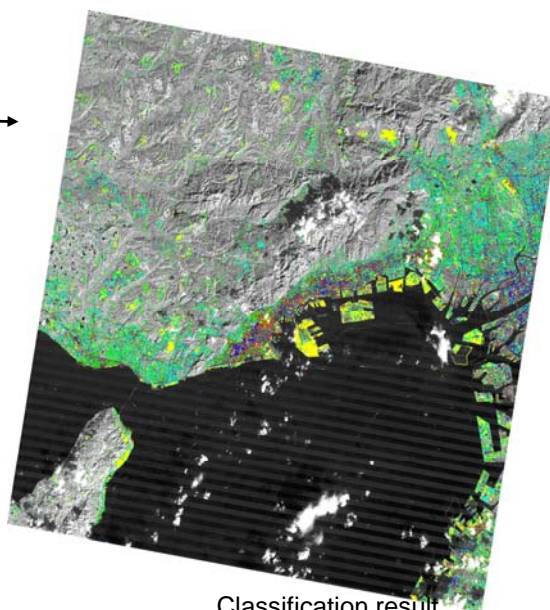
Black: damaged building  
 Threshold values are same as the  
 Kobe earthquake



# Damage Detection Using Supervised Classification



Maximum Likelihood Classification



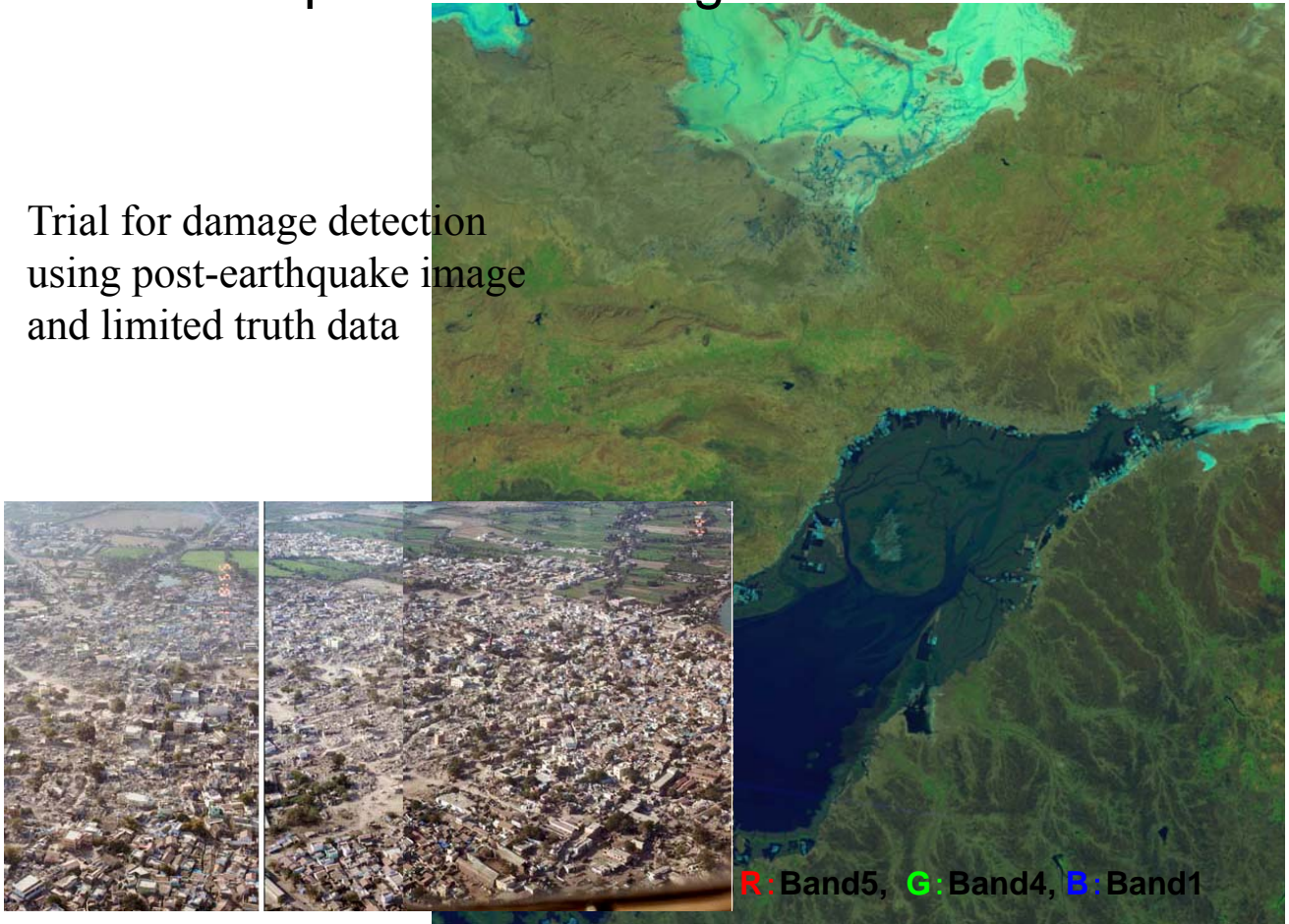
Classification result

Spectral changes of damaged areas



# Supervised Damage Estimation

Trial for damage detection using post-earthquake image and limited truth data



# Maximum Likelihood Classification

